Electronic Supplementary Material (ESI) for Dalton Transactions.
This journal is © The Royal Society of Chemistry 2017

Heterodinuclear Titanium/Zinc Catalysis: Synthesis, Characterization and Activity for CO_2/Epoxide Copolymerization and Cyclic Ester Polymerization

Jennifer A. Garden,[a] Andrew J. P. White,[b] Charlotte K. Williams*[c]

[a] EastCHEM School of Chemistry, Joseph Black Building, University of Edinburgh, David Brewster Road, Edinburgh EH9 3FJ, UK

[b] Department of Chemistry, Imperial College London, London, SW7 2AZ, UK

[c] Department of Chemistry, Mansfield Road, University of Oxford, Oxford, OX1 3TA, UK

charlotte.williams@chem.ox.ac.uk

Table of Contents

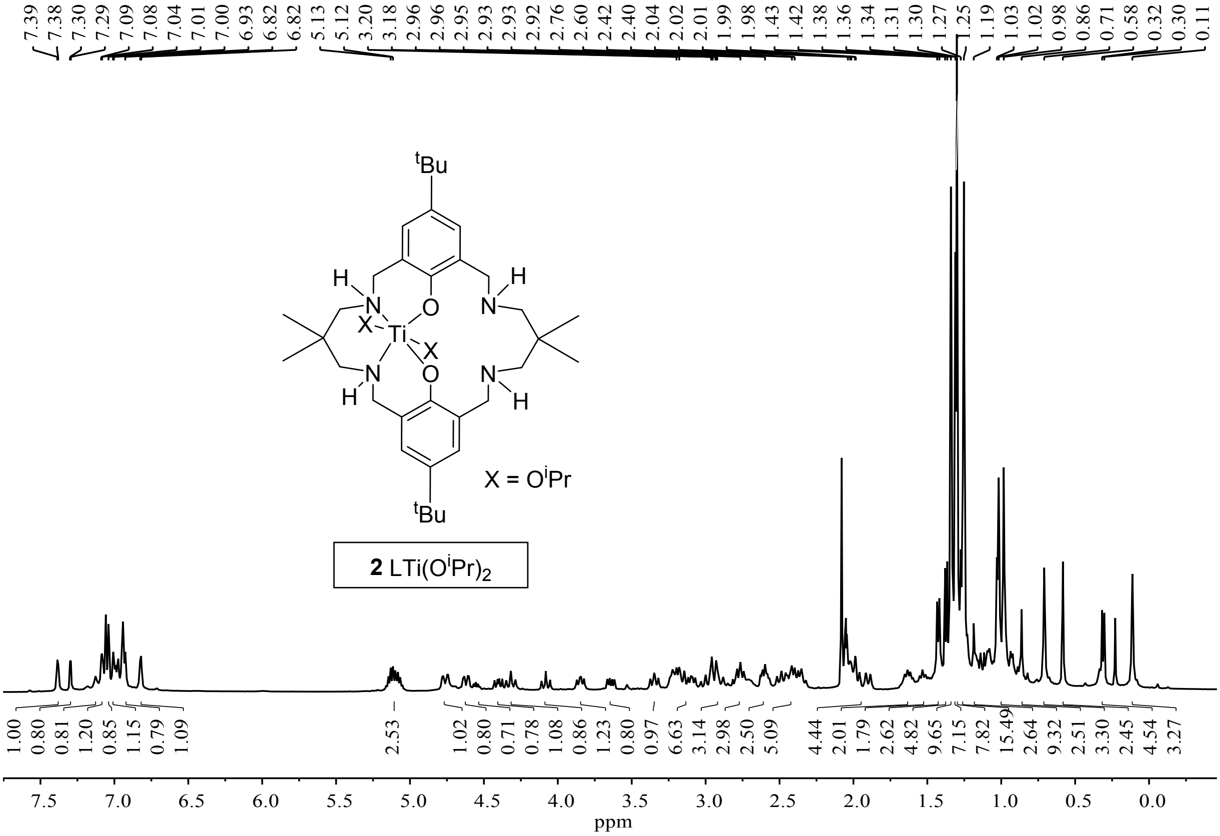

Figure S1: ^{1}H NMR spectrum of LTi(O^{i}Pr)$_2$ in d$_8$-toluene solvent, at 298 K.

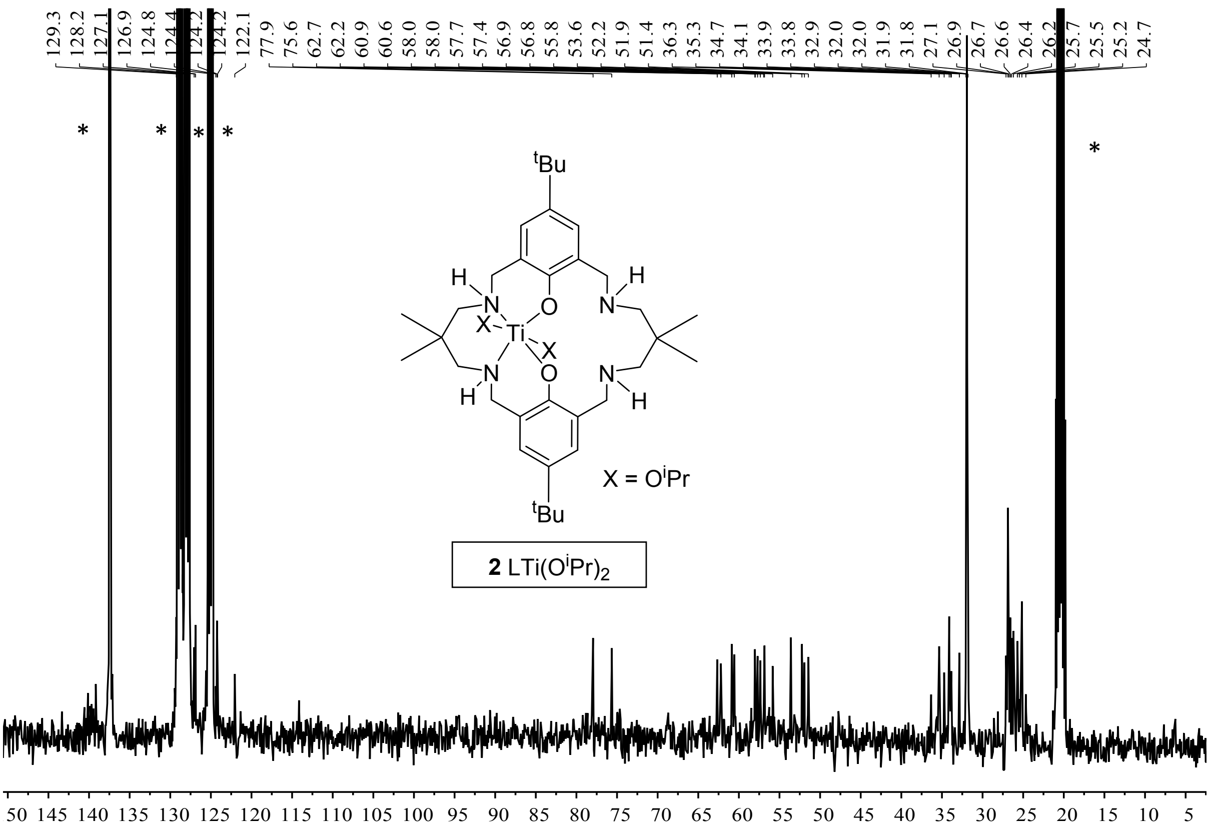

Figure S2: ^{13}C NMR spectrum of LTi(O^{i}Pr)$_2$ in d$_8$-toluene solvent, at 298 K.

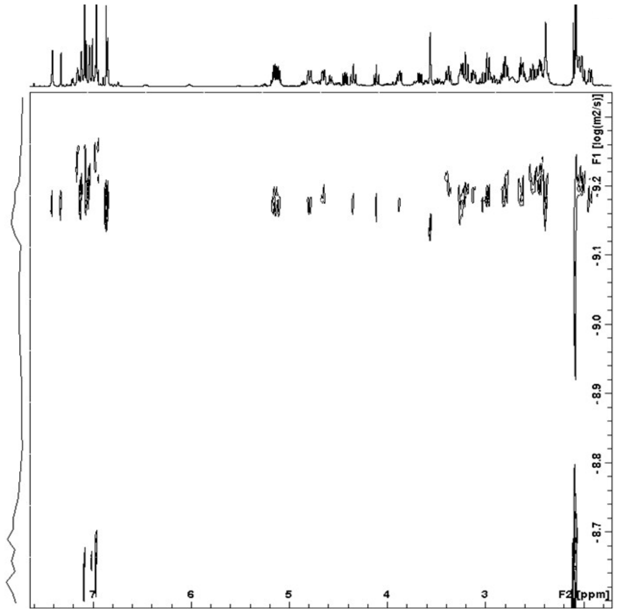

Figure S3 DOSY NMR spectrum of LTi(O^{i}Pr)$_2$ in d$_8$-toluene at 298K.

Comparison of the diffusion coefficient obtained experimentally for LTi(O^{i}Pr)$_2$ (logD = -9.177), to the calibration plot, yielded a predicted molecular weight of 614 g mol^{-1} for the species present in solution. This value lies close to that of LTi(O^{i}Pr)$_2$, which would have a molecular weight of 716 g mol^{-1}, giving a 86% agreement which lies within the error range typically expected for DOSY analysis.

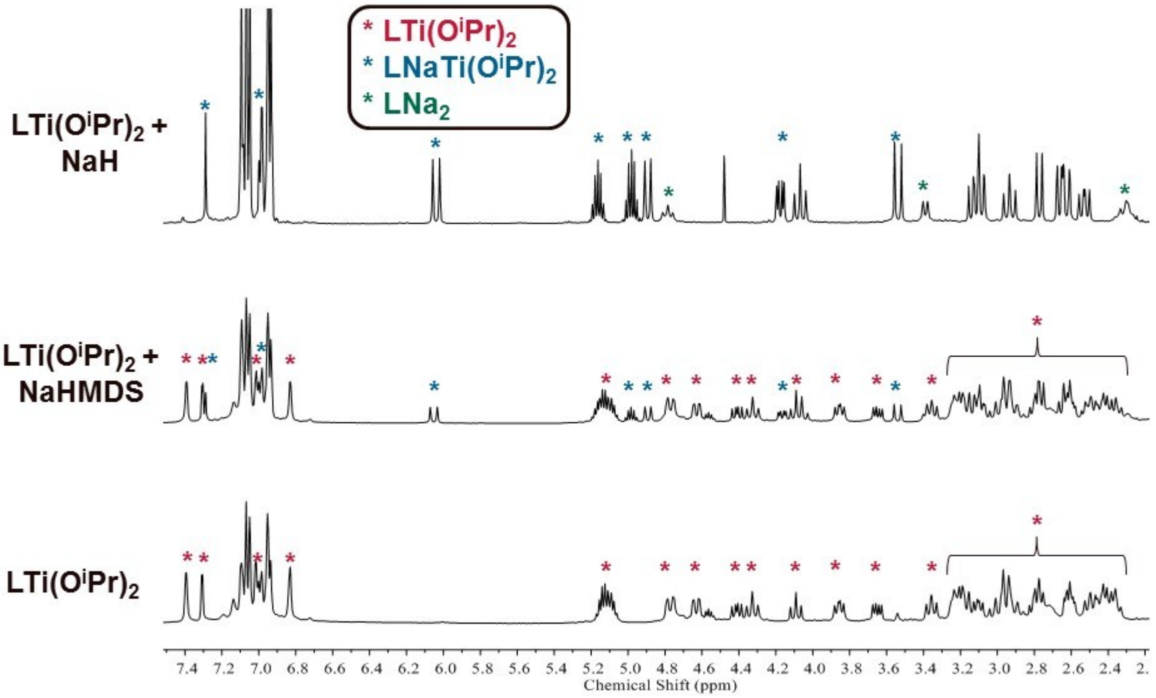

Figure S4 Overlaid spectra of LTi(O^{i}Pr)$_2$ (bottom) and the *in situ* reaction with NaHMDS (middle) or NaH (top), to form LNaTi(O^{i}Pr)$_2$, along with LNa$_2$ and unreacted LTi(O^{i}Pr)$_2$, in d$_8$-toluene solvent, at 298K.

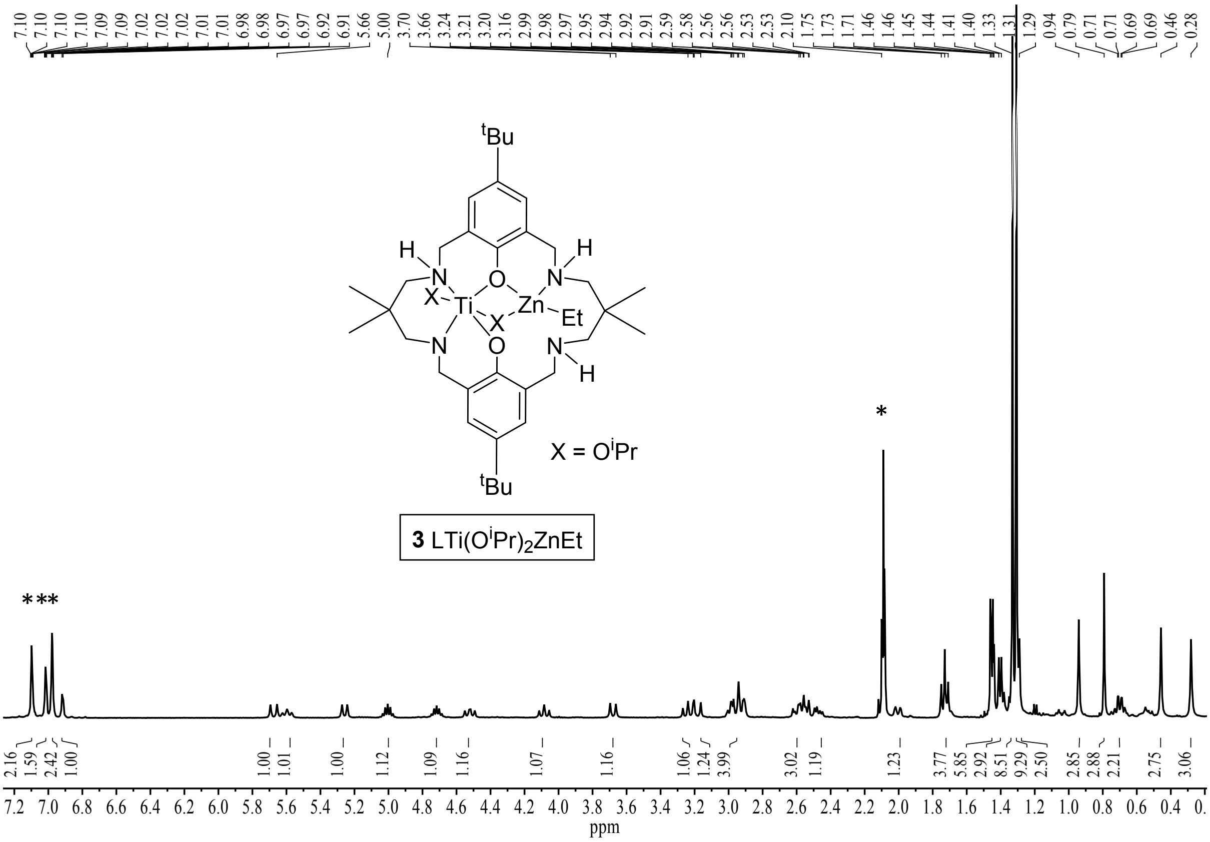

Figure S5: ^{1}H NMR spectrum of LTi(O^{i}Pr)$_2$ZnEt in d$_8$-toluene solvent, at 298 K.

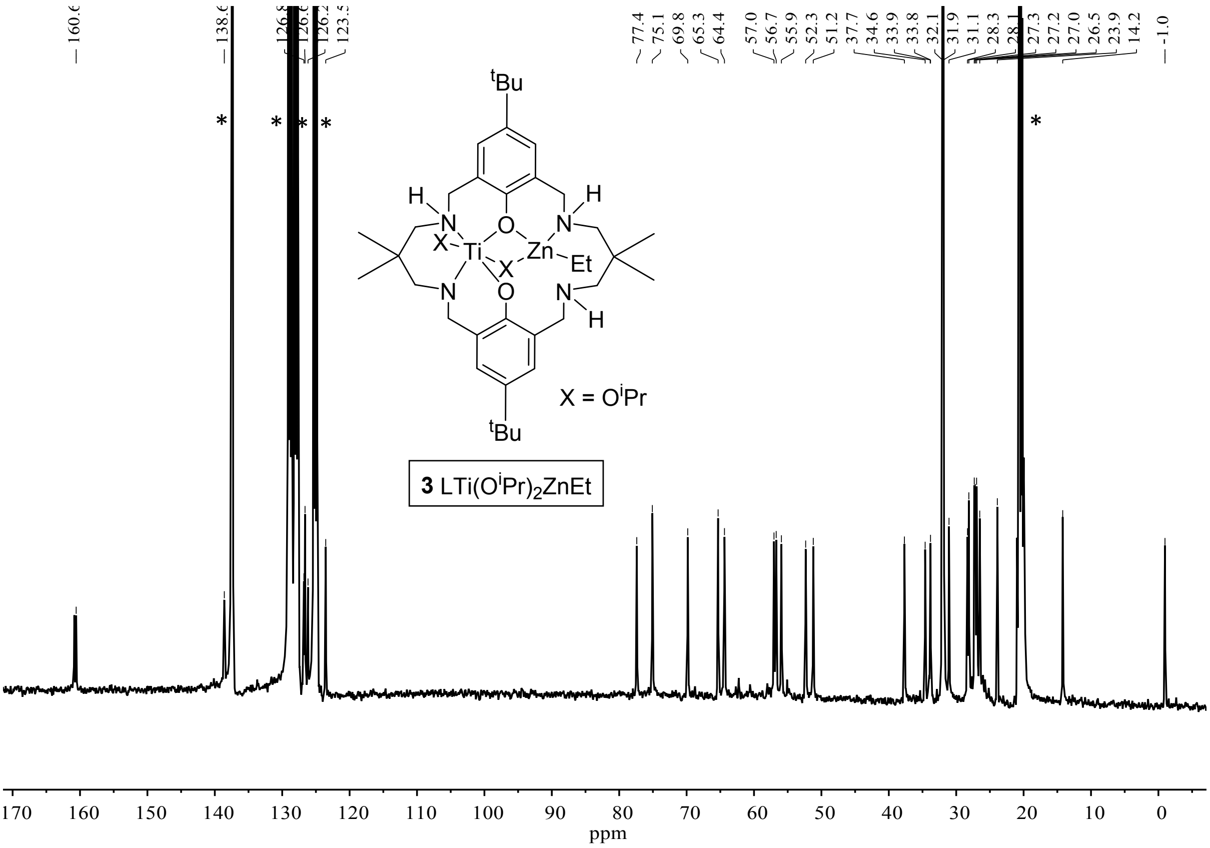

Figure S6: ^{13}C NMR spectrum of LTi(O^{i}Pr)$_2$ZnEt in d$_8$-toluene solvent, at 298 K.

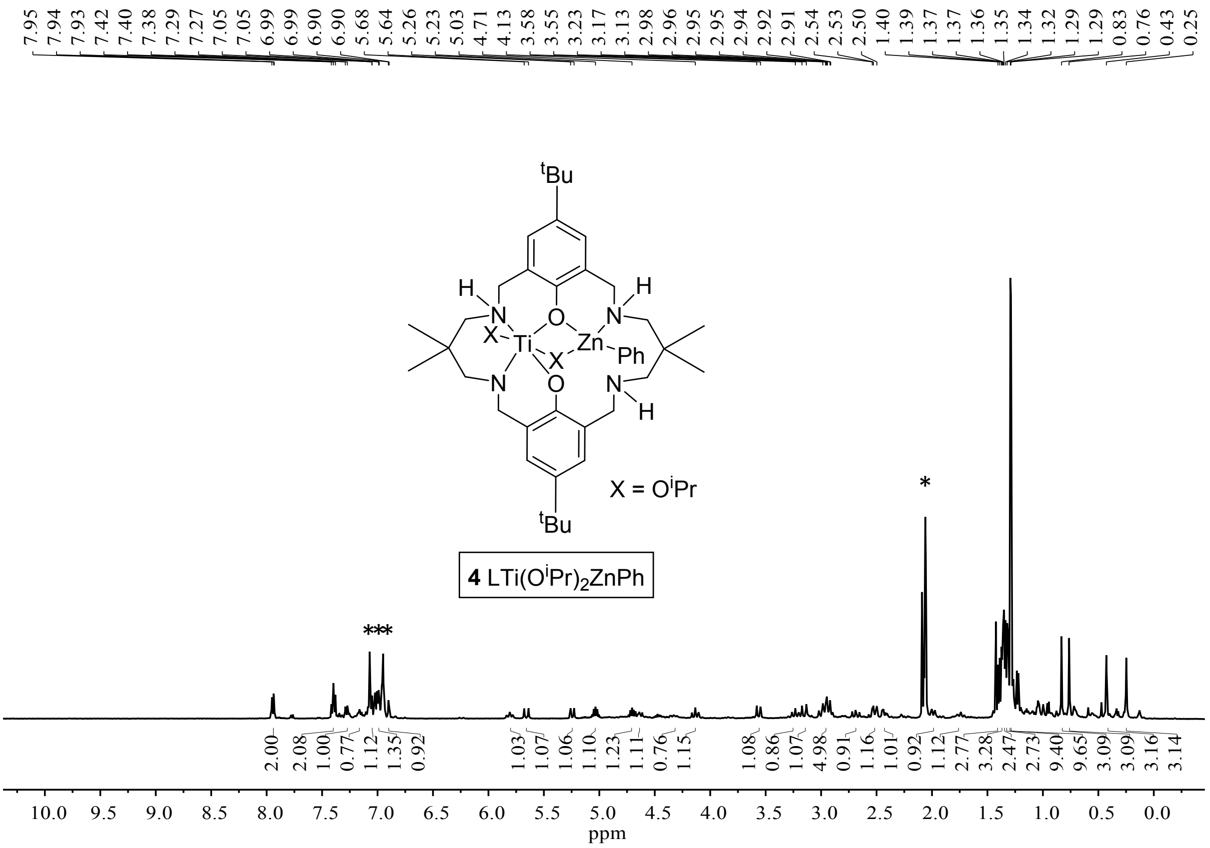

Figure S7: ^{1}H NMR spectrum of LTi(O^{i}Pr)$_2$ZnPh in d$_8$-toluene solvent, at 298 K.

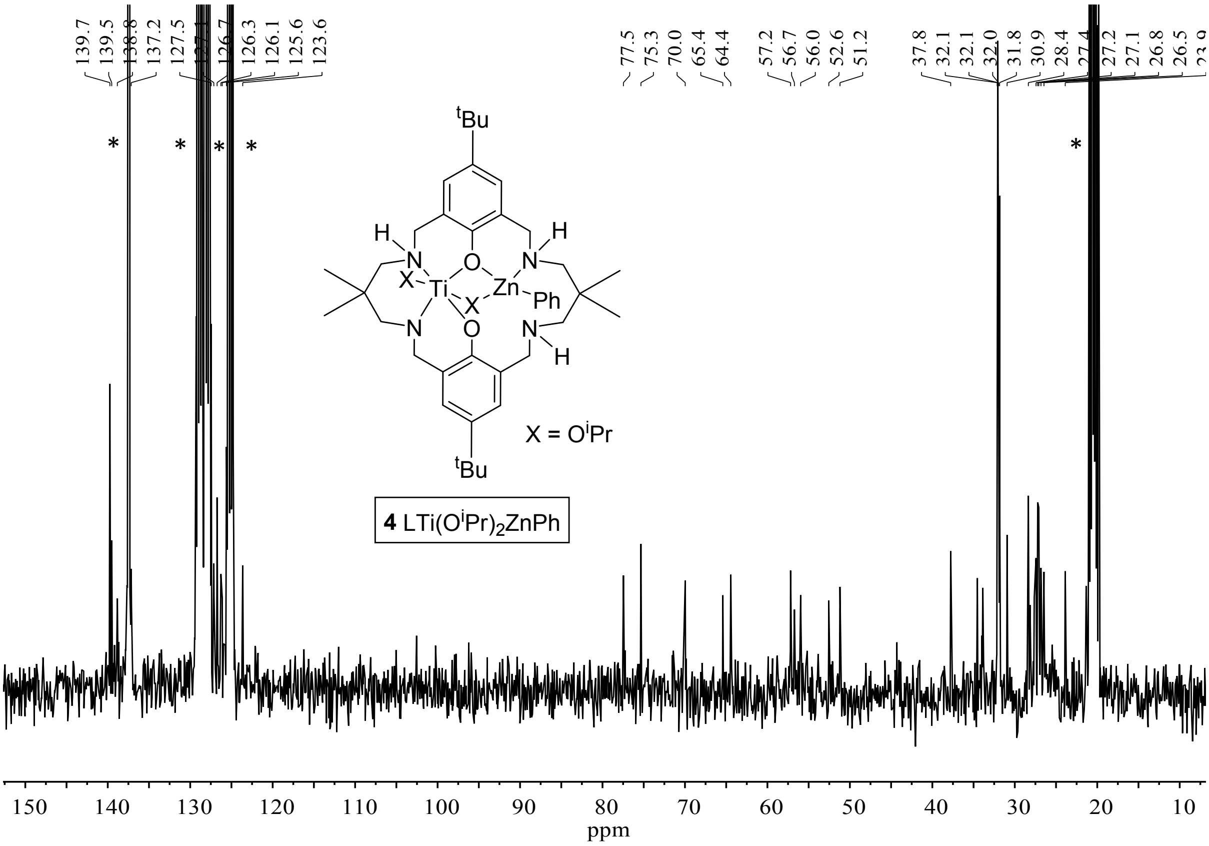

Figure S8: ^{13}C NMR spectrum of LTi(O^{i}Pr)$_2$ZnPh in d$_8$-toluene solvent, at 298 K.

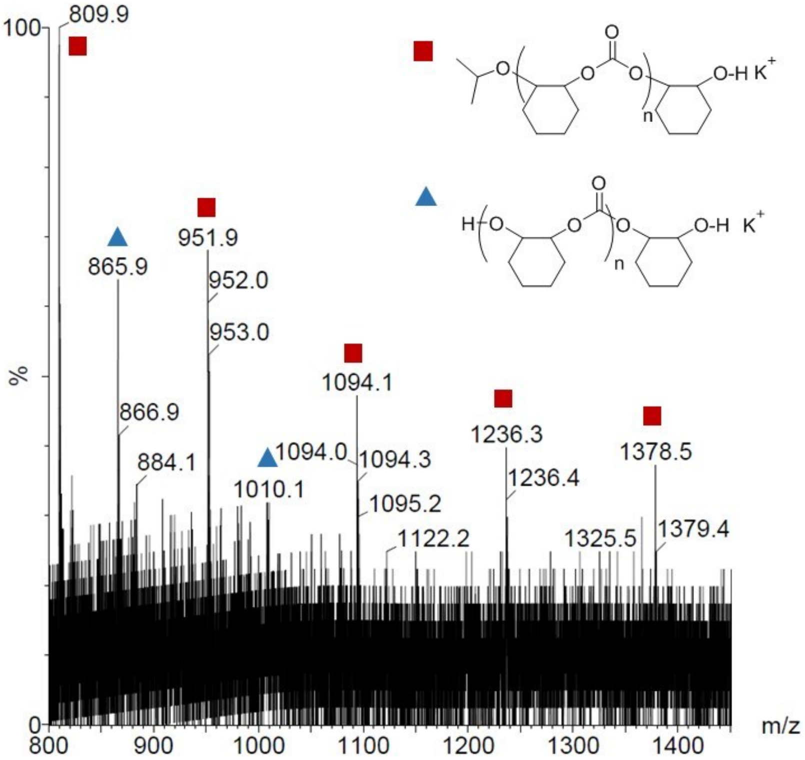

Figure S9: MALDI-ToF mass spectra of PCHC produced with LTi(O^{i}Pr)$_2$ZnEt.

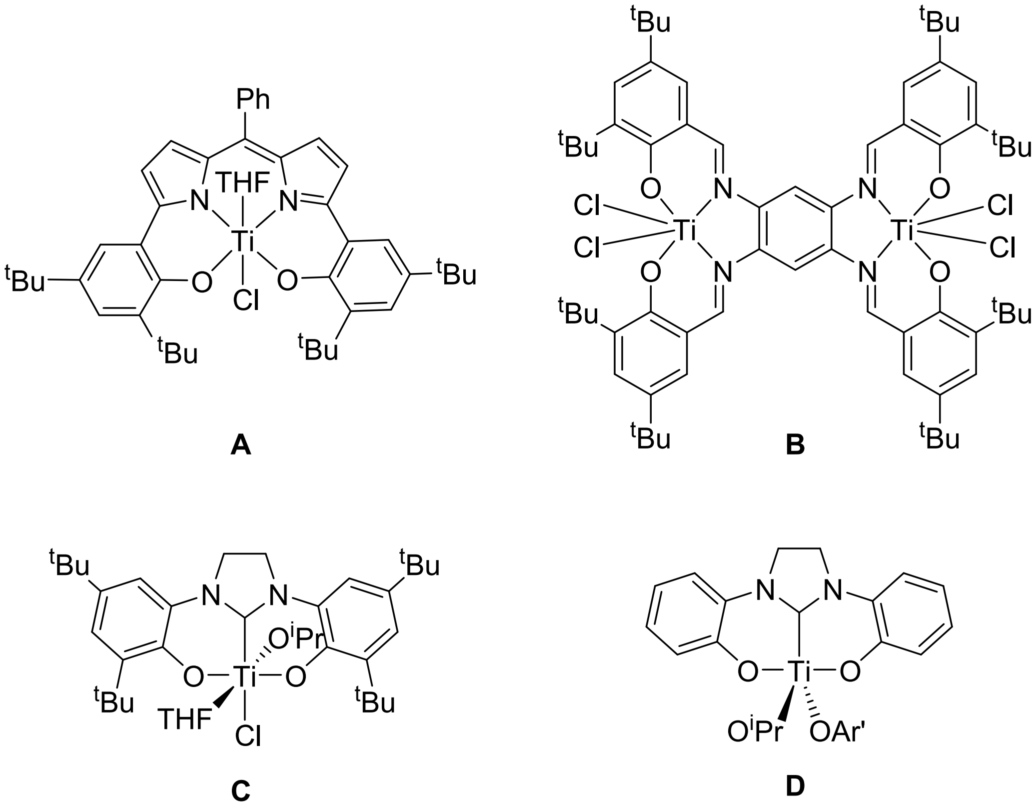

Figure S10: Illustrates the structures of the titanium (IV) diphenolate catalyst (**A**, top left), the titanium (IV) bis(salphen) catalyst (**B**, top right) and the titanium (IV) N-heterocyclic carbene catalysts (**C** and **D**, bottom).

Table S1 CO_2/CHO ROCOP data for runs using titanium *iso*-propoxide literature reported catalysts (**A-C**) and complexes **3** and **4**.

Cat.	**Additive (cat:additive)**	**Cat. Loading (mol%)**	**Time (h)**	**CO_2 Pressure (bar)**	**Temp. (°C)**	**Conv. (%)**	**TOF (h^{-1})**	**CO_2 (%)**	**M_n [Đ]**
A[1]	[PPN]Cl (1:1)	0.05	12	20	60	45	76	99	13000 [1.27]
B[2]	TBAB (1:1)	0.1	6	35	50	95	123	74	9130 [1.14]
C[3]	[PPN]Cl (1:1)	0.04	24	10	60	44	46	>99	13800 [1.38]
D[4]	[PPN]Cl (1:1)	0.04	24	< 1	60	6	6	>99	-
D[4]	[PPN]N_3 (1:1)	0.04	24	< 1	60	8	8	>99	-
3	-	1	6	1	80	18	3	>99	-
3	-	1	24	1	80	53	2	94	2190 [1.35]
4	-	1	6	1	80	23	4	95	-
4	-	1	24	1	80	40	2	98	1750 [1.37]

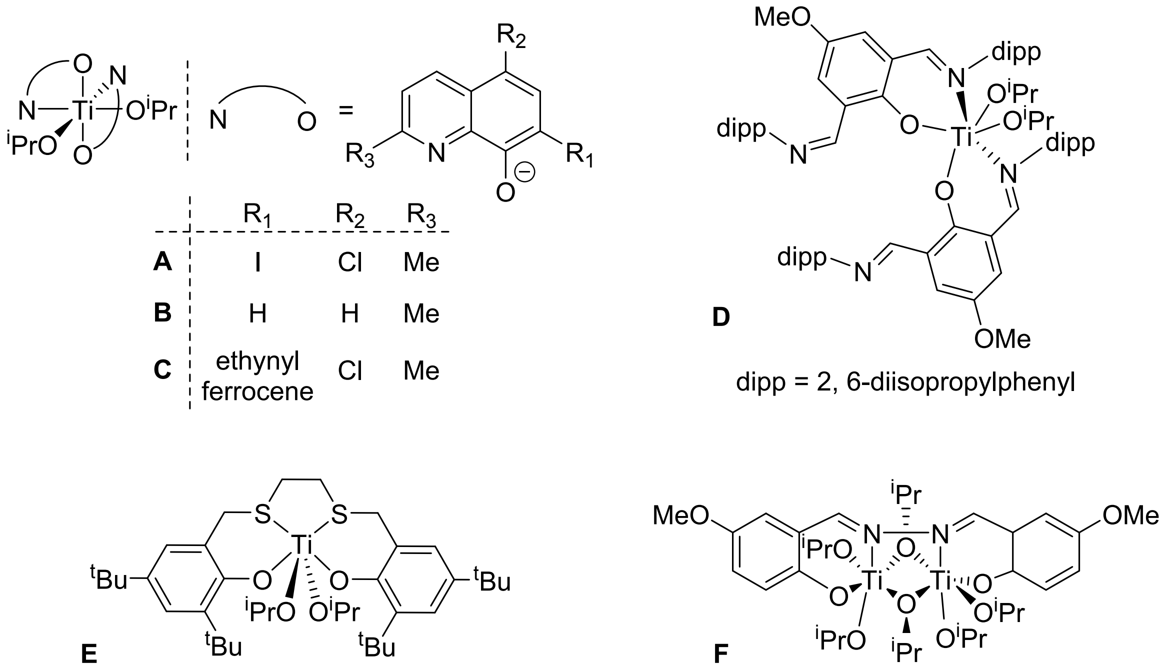

Figure S11. Illustrates the structures of literature reported catalysts **A-F** (refer to Table S2).

Table S2. Results for ROP of lactide using titanium *iso*-propoxide literature reported catalysts (**A-F**) and complexes **3** and **4**.

Cat.	**Additive (cat:additive)**	**[LA] (M)**	**Solvent**	**Temp. (°C)**	**Cat. Loading (mol%)**	**k_{obs} (reported)**	**k_{obs} (s^{-1})**
A[5]	^{i}PrOH (1:1)	1	toluene	75	1	3.7×10^{-6} s^{-1}	3.7×10^{-6} s^{-1}
B[5]	^{i}PrOH (1:1)	1	toluene	75	1	2.0×10^{-6} s^{-1}	2.0×10^{-6} s^{-1}
C[5]	^{i}PrOH (1:1)	1	toluene	75	1	1.7×10^{-6} s^{-1}	1.7×10^{-6} s^{-1}
D[6]	N/A	-	neat	130	0.5	0.61 min^{-1}	10.2×10^{-3} s^{-1}
E[7]	N/A	0.5	benzene	100	1	16×10^{-3} h^{-1}	4.4×10^{-6} s^{-1}
F[8]	N/A	2	toluene	60	1	94.2×10^{-3} min^{-1}	15.7×10^{-4} s^{-1}
3	N/A	1	THF	70	1	10.8×10^{-4} s^{-1}	10.8×10^{-4} s^{-1}
4	N/A	1	THF	70	1	6.3×10^{-4} s^{-1}	6.3×10^{-4} s^{-1}

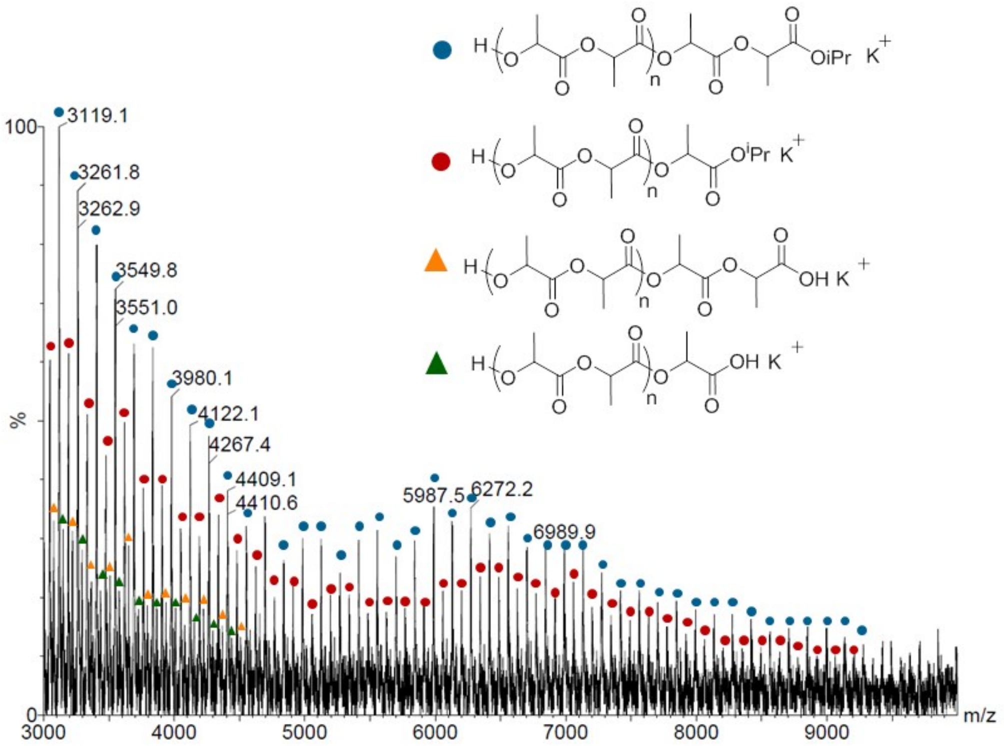

Figure S12. MALDI-ToF spectrum of polylactide produced using LTi(O^{i}Pr)$_2$ZnEt.

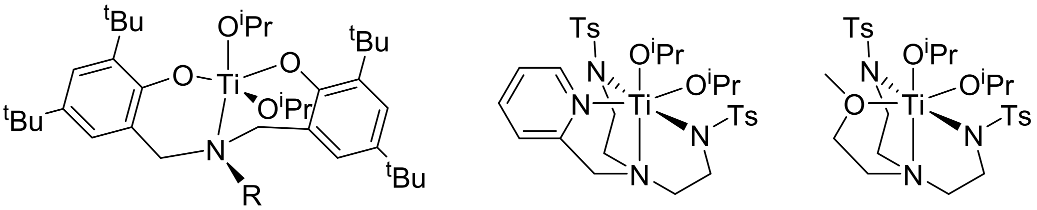

A: R = ^{i}Pr
B: R = ^{n}Pr

C

D

Figure S13. Illustrates the structures of literature reported catalysts **A-D** (refer to Table S3).

Table S3. Results for ROP of ε-caprolactone using titanium *iso*-propoxide literature reported catalysts (**A-D**) and complexes **3** and **4**.

Cat.	[ε-CL] (M)	Solvent	Temp. (°C)	Cat. Loading (mol%)	k_{obs} (reported)	k_{obs} (s^{-1})
A[9]	1.807	toluene	25	1	4.88×10^{-6} s^{-1}	4.9×10^{-6}
B[9]	1.807	toluene	25	1	7.54×10^{-5} s^{-1}	7.5×10^{-5}
C[10]	1.0	toluene	100	1	7.5×10^{-3} min^{-1}	1.3×10^{-4}
D[10]	1.0	toluene	100	1	6.5×10^{-2} min^{-1}	10.8×10^{-4}
3	0.9	THF	70	1	5.2 x x10^{-4} s^{-1}	5.2 x x10^{-4}
4	0.9	THF	70	1	4.6 x x10^{-4} s^{-1}	4.6 x x10^{-4}

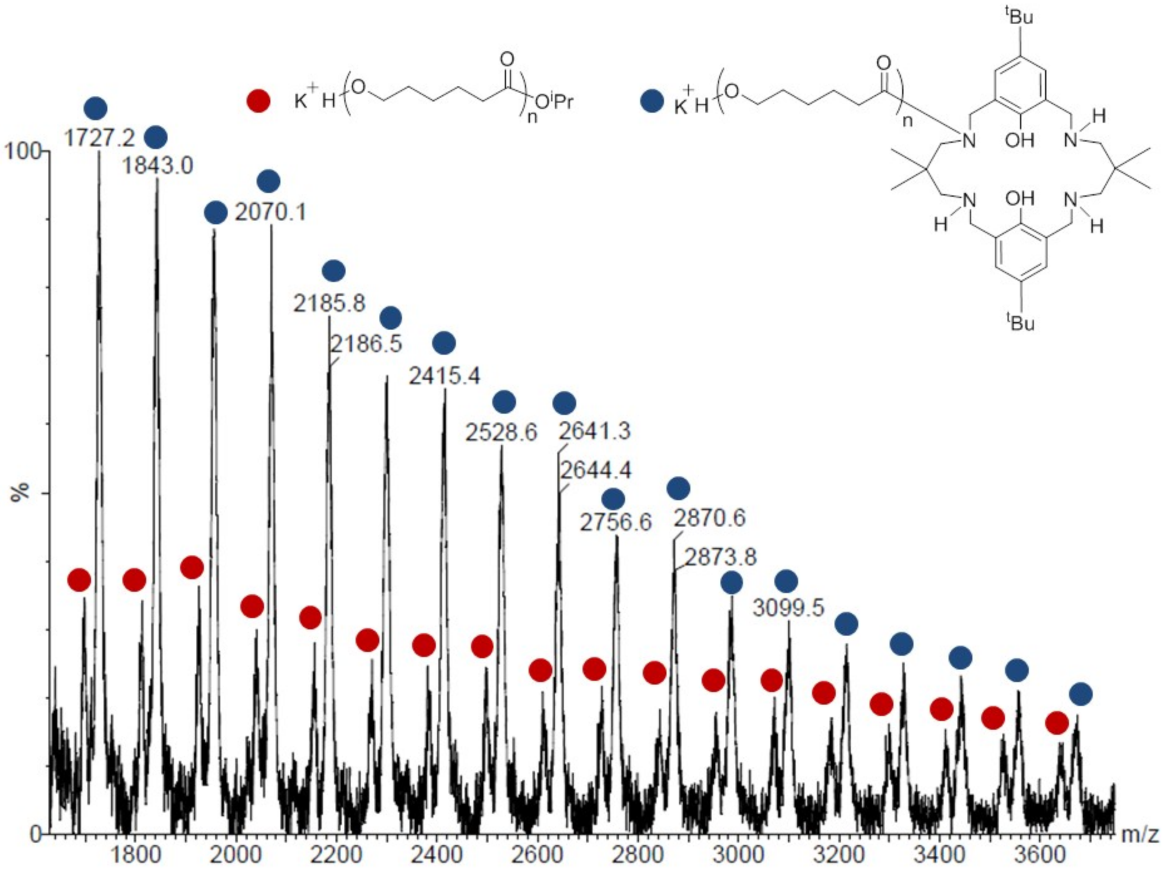

Figure S14. MALDI-ToF mass spectra of polycaprolactone produced with LTi(O^{i}Pr)$_2$ZnEt.

Polymerization Studies

CHO-CO_2 Copolymerization Reactions

The catalyst LTi(O^{i}Pr)$_2$ZnEt (99 µmol , 80 mg) was placed in a Schlenk tube in the glovebox and CHO (9.9 mmol, 1.0 mL) was added. The reaction mixture was subsequently de-gassed and then heated to 80 °C at 1 bar CO_2 pressure. The reaction mixture was quenched by exposure to air and a ^{1}H NMR spectrum of the crude reaction mixture was recorded in $CDCl_3$ solvent. Unreacted CHO was removed *in vacuo* and the product polycarbonate was then purified through dissolution in THF followed by precipitation from pentane.

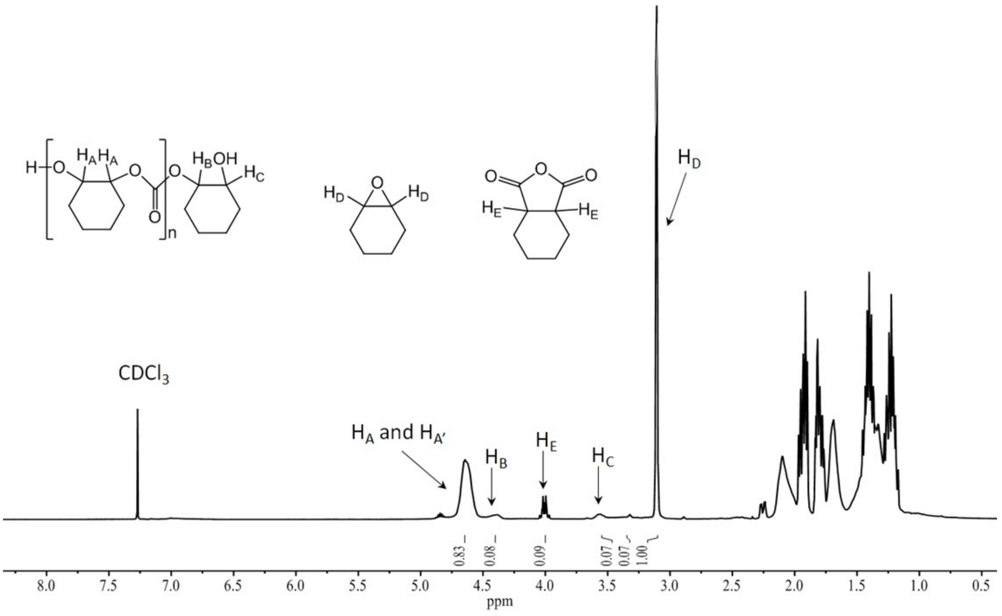

Figure S15. ^{1}H NMR spectrum of crude PCHC sample produced with LTi(O^{i}Pr)$_2$ZnEt, in $CDCl_3$ at 298 K, showing formation of PCHC (4.68 ppm) with ether linkages (3.4 ppm) and cyclic carbonate (4.1 ppm) by-products.

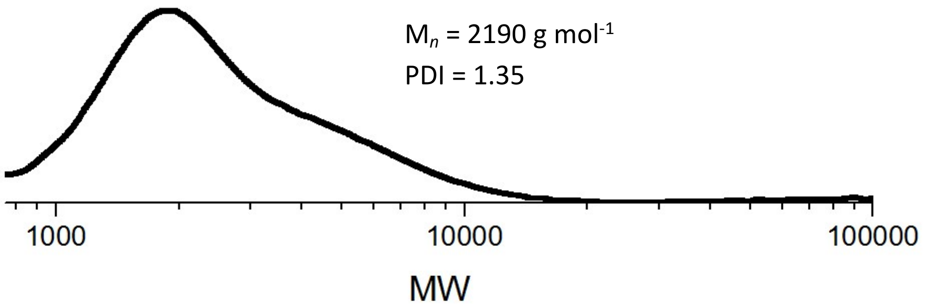

Figure S16. SEC plot of Mw for the PCHC formed by LTi(O^{i}Pr)$_2$ZnEt.

Lactide Polymerization Reactions

Under a nitrogen atmosphere in the glovebox, LTi(O^{i}Pr)$_2$ZnEt (8.1 mg, 0.01 mmol) was added to a screw capped vial, followed by a 1M solution of L-lactide in THF (144 mg, 1 mmol in 1 mL). The polymers were purified through recrystallization from THF/methanol.

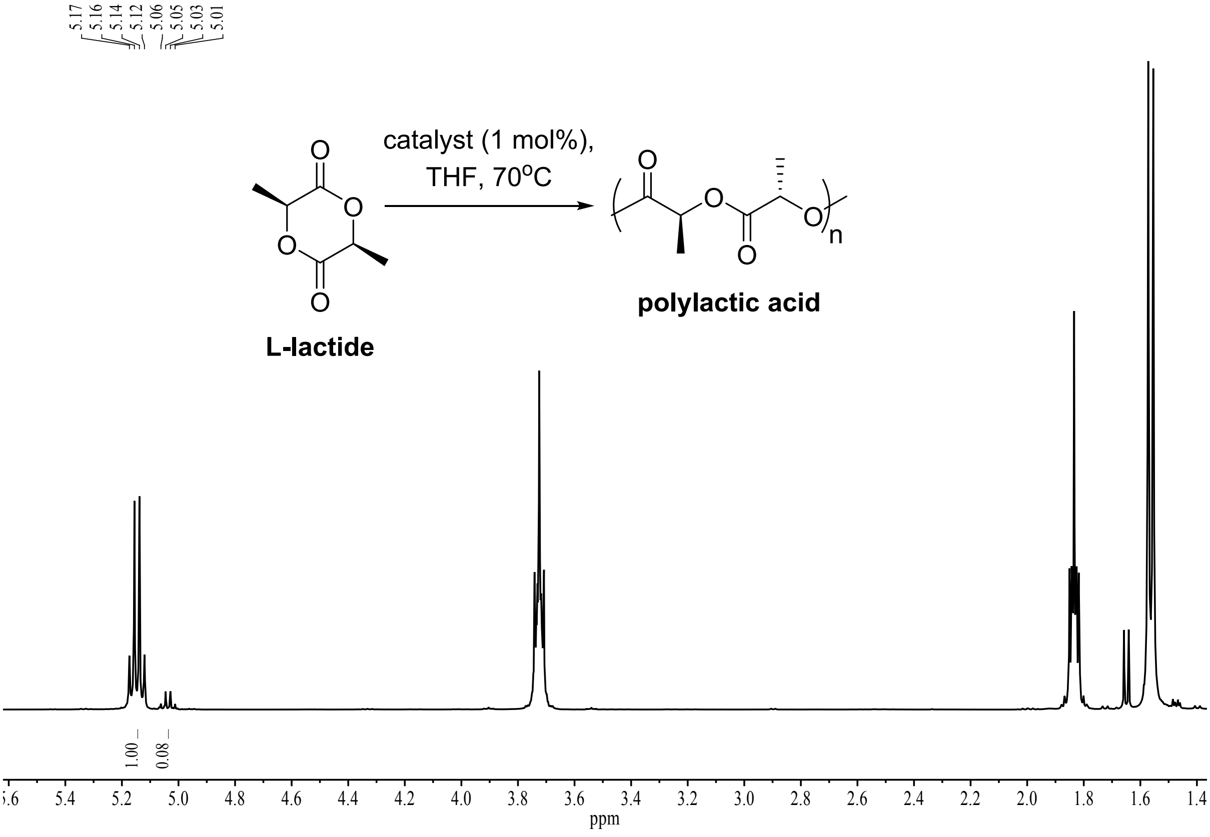

Figure S17. Expanded ^{1}H NMR spectrum of the crude L-lactide polymerization reaction mixture in $CDCl_3$ at 298K, showing the polylactide (5.15 ppm) and L-lactide (5.04 ppm) signals used to calculate the TON and TOF number achieved by the catalyst.

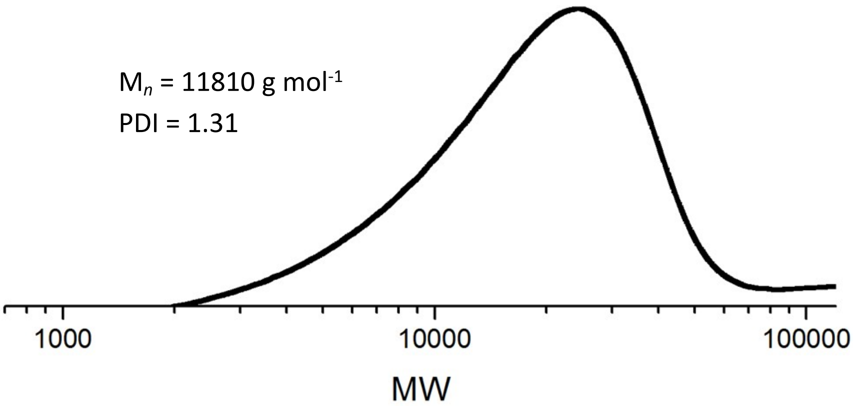

Figure S18. SEC plot of Mw for the polylactide formed by LTi(O^{i}Pr)$_2$ZnEt.

ε-Caprolactone Polymerization Reactions

Under a nitrogen atmosphere in a glovebox, ε-caprolactone (0.11 mL, 1 mmol), THF (1 mL) and LTi(O^{i}Pr)$_2$ZnEt (8.1 mg, 0.01 mmol) were added to a screw vial. The reaction was then stirred at 21°C or 70 °C. The polymerization was quenched by the addition of hexane, and the product was purified by dissolution in THF, then precipitation from methanol to afford a white powder.

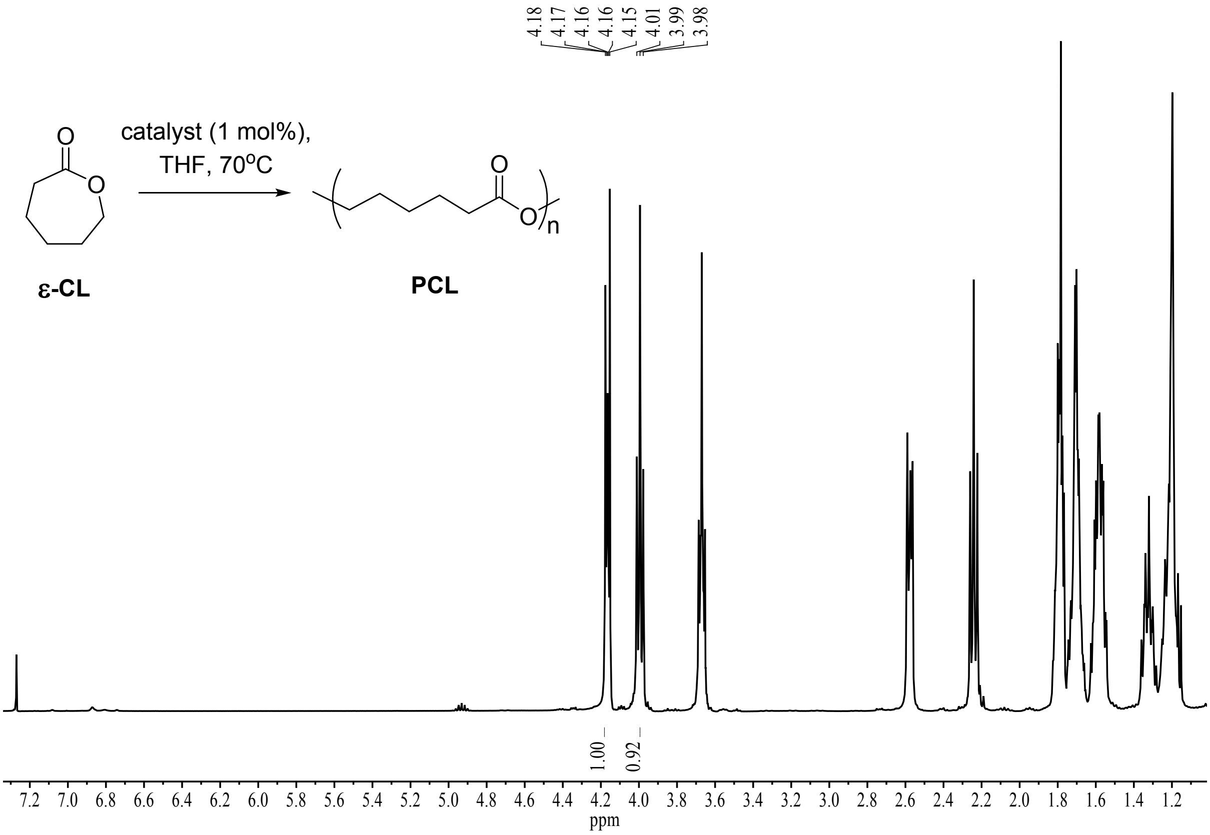

Figure S19. Expanded ^{1}H NMR spectrum of the crude ε-caprolactone polymerization reaction mixture in $CDCl_3$ at 298K, showing the polycaprolactone (4.08 ppm) and ε-caprolactone (4.26 ppm) signals used to calculate the TON and TOF number achieved by the catalyst.

DOSY NMR Studies

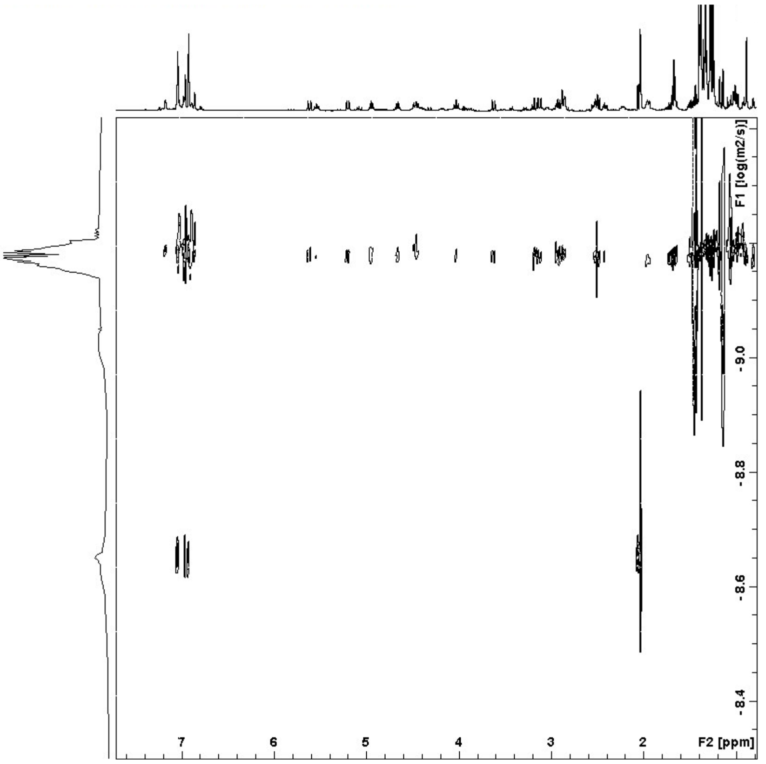

Figure S20. DOSY NMR spectrum of LTi(O^{i}Pr)$_2$ZnEt in d$_8$-toluene.

Comparison of the diffusion coefficient obtained experimentally for LTi(O^{i}Pr)$_2$ZnEt (logD = -9.179), to the calibration plot, yielded a predicted molecular weight of 711 g mol^{-1} for the species present in solution. This value lies close to that of LTi(O^{i}Pr)$_2$ZnEt, which would have a molecular weight of 808 g mol^{-1}, giving an 88% agreement which lies within the error range typically expected for DOSY analysis.

Instrument Details

The Diffusion-Ordered Spectroscopy (DOSY) NMR experiments were performed at 298K on a Bruker 500 AVANCE III HD NMR spectrometer operating at a frequency of 500.13 MHz for proton resonance under TopSpin (version 3.2, Bruker Biospin, Karlsruhe) and equipped with a z-gradient bbfo/5mm tuneable "SmartProbe"™ probe and a GRASP II gradient spectroscopy accessory providing a maximum gradient output of 53.5 G/cm (5.35G/cmA).

Diffusion ordered NMR data was acquired using the Bruker pulse program ledbpgp2s with a spectral width of 5500Hz (centred on 4.5 ppm) and 32768 data points.[11] A relaxation delay of 12 s was employed along with a diffusion time (large delta) of 100 ms and a longitudinal eddy current delay (LED) of 5 ms. Bipolar gradients pulses (little delta/2) of 2.2 ms and homospoil gradient pulses of 0.6 ms were used. The gradient strengths of the 2 homospoil pulses were -17.13% and -13.17%. 32 experiments were collected with the bipolar gradient strength, initially at 2% (1st experiment), linearly increased to 95% (32nd experiment). All gradient pulses were smooth-square shaped (SMSQ10.100) and after each application a recovery delay of 200 µs used. The experiment was run with 24 scans per increment, employing one stimulated echo with two spoiling gradients.

DOSY plots were generated by using the DOSY processing module of TopSpin. Parameters were optimized empirically to find the best quality of data for presentation purposes. Diffusion coefficients were calculated by fitting intensity data to the Stejskal-Tanner expression.

Preparation of External Calibration Plots

A calibration plot was formed through DOSY analysis of a range of standards spanning the molecular weight range of 161.4 to 643.4 g mol^{-1} [hexamethyldisilazane (HMDSH), 161.4; Zn(HMDS)$_2$, 386.2; β-diketiminate ligand HC(C(Me)N-2,6-^{i}Pr$_2$C$_6$H$_3$)$_2$, (BDIH), 418.7; (BDI)Zn(HMDS), 643.4 g mol^{-1}, Table S4]. From the diffusion coefficients of the external standards, linear calibration graphs were obtained by plotting logD vs logMW (Graph S1). Following DOSY analysis of the product (i.e. LTi(O^{i}Pr)$_2$ZnEt), the diffusion coefficient obtained for the signals corresponding to the product allowed an estimate of the MW of the species present in solution.

Table S4. Diffusion coefficients of standards in d$_8$-toluene solution compared to their molecular weight.

Compound	LogD	MW (g mol^{-1})	LogMW
d$_8$-toluene	-8.702	100.2	2.0008
HMDSH	-8.850	161.4	2.2079
Zn(HMDS)$_2$	-9.039	386.2	2.5868
(BDI)Zn(HMDS)	-9.182	643.4	2.8085

Graph S1. LogD vs LogMW representation from the ^1H DOSY NMR data obtained for shows the standards HMDSH, $Zn(HMDS)_2$ and (BDI)Zn(HMDS) in d_8-toluene solvent.

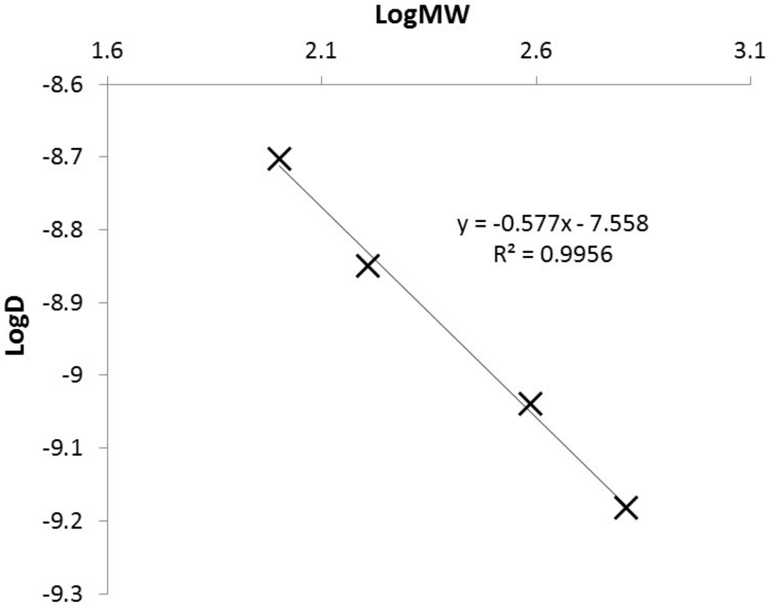

Xray Crystallographic Data

The X-ray crystal structure of 3

Crystal data for **3**: $C_{42}H_{72}N_4O_4TiZn$, M = 810.30, triclinic, P-1 (no. 2), a = 12.0895(5), b = 13.3126(5), c = 14.0794(6) Å, α = 82.118(3), β = 73.055(4), γ = 85.369(3)°, V = 2145.13(15) Å^3, Z = 2, D_c = 1.255 g cm^{-3}, μ(Mo-Kα) = 0.788 mm^{-1}, T = 173 K, orange plates, Agilent Xcalibur 3E diffractometer; 8462 independent measured reflections (R_{int} = 0.0197), F^2 refinement,[12, 13] R_1(obs) = 0.0466, wR_2(all) = 0.1099, 6525 independent observed absorption-corrected reflections [$|F_o| > 4\sigma(|F_o|)$, $2\theta_{full}$ = 50°], 514 parameters. CCDC 1507078.

The C24-based *t*-butyl group and the C50-based ethyl ligand in the structure of **3** were both found to be disordered. In each case two orientations were identified (of *ca*. 62:38 and 78:22% occupancy), their geometries were optimized, the thermal parameters of adjacent atoms were restrained to be similar, and only the non-hydrogen atoms of the major occupancy orientations were refined anisotropically (those of the minor occupancy orientations were refined isotropically). The N–H hydrogen atoms on N4, N14 and N18 were located from ΔF maps and refined freely subject to an N–H distance restraint of 0.90 Å.

The X-ray crystal structure of 4

Crystal data for **4**: $C_{46}H_{72}N_4O_4TiZn{\cdot}C_6H_{14}$, M = 944.51, monoclinic, $P2_1/n$ (no. 14), a = 15.53237(14), b = 19.46458(16), c = 17.75532(16) Å, β = 102.0062(9)°, V = 5250.56(8) Å^3, Z = 4, D_c = 1.195 g cm^{-3}, μ(Cu-Kα) = 2.196 mm^{-1}, T = 173 K, yellow blocks, Agilent Xcalibur PX Ultra A diffractometer; 10169 independent measured reflections (R_{int} = 0.0319), F^2 refinement, [12, 13] R_1(obs) = 0.0374, wR_2(all) = 0.1024, 8422 independent observed absorption-corrected reflections [$|F_o| > 4\sigma(|F_o|)$, $2\theta_{full}$ = 135°], 621 parameters. CCDC 1507079.

The O45-based *iso*-propyl group and the C61-based included hexane solvent molecule in the structure of **4** were both found to be disordered. For the former two orientations for the $C(H)Me_2$ unit were identified of *ca*. 80 and 20% occupancy, whilst for the latter two orientations for the complete molecule were identified of *ca*. 67 and 33% occupancy. In each case the geometries of the two orientations were optimized, the thermal parameters of adjacent atoms were restrained to be similar, and only the non-hydrogen atoms of the major occupancy orientations were refined anisotropically (those of the minor occupancy orientations were refined isotropically). The N–H hydrogen atoms on N4, N14 and N18 were located from ΔF maps and refined freely subject to an N–H distance restraint of 0.90 Å.

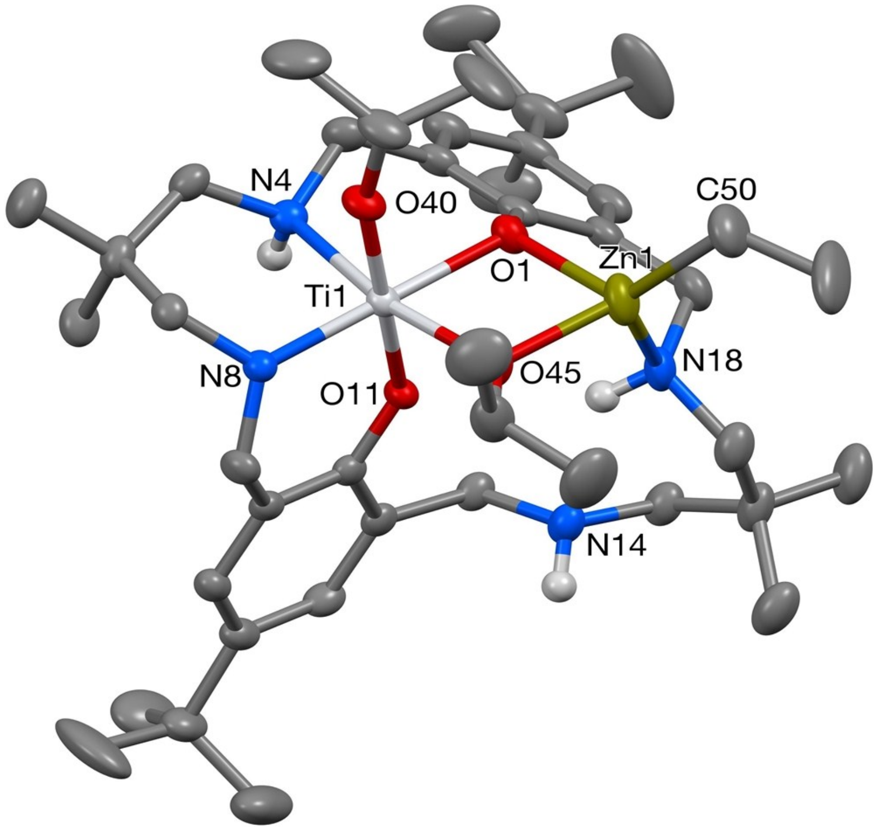

Figure S21. The crystal structure of **3** (50% probability ellipsoids).

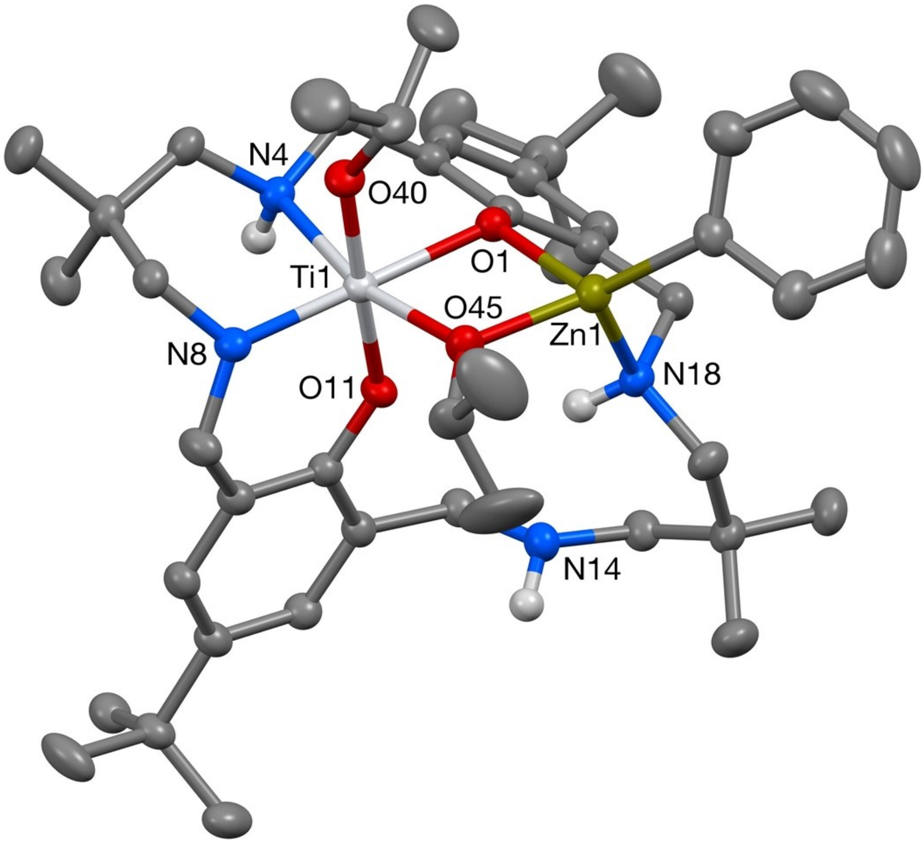

Figure S22. The crystal structure of **4** (50% probability ellipsoids).

Determination of dn/dc from RI

Graph S2. Determination of dn/dc for polycaprolactone (dn/dc = 0.078)

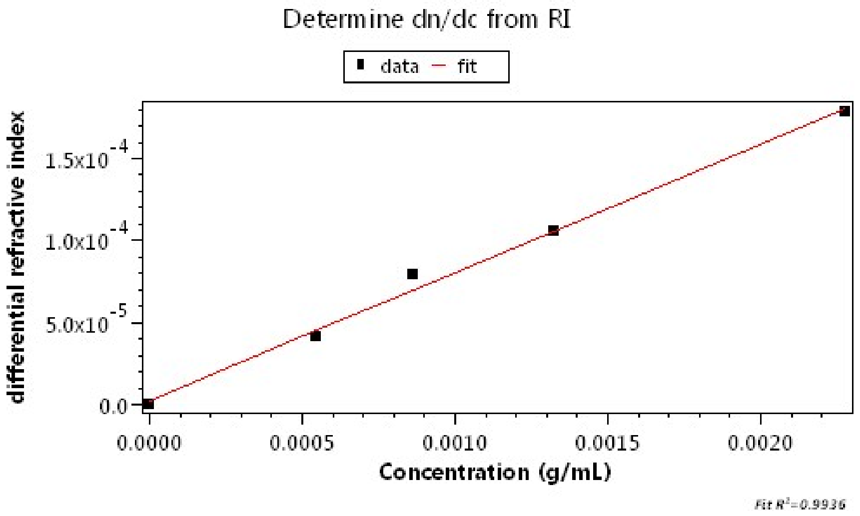

Graph S3. Determination of dn/dc for polylactide (dn/dc = 0.05)

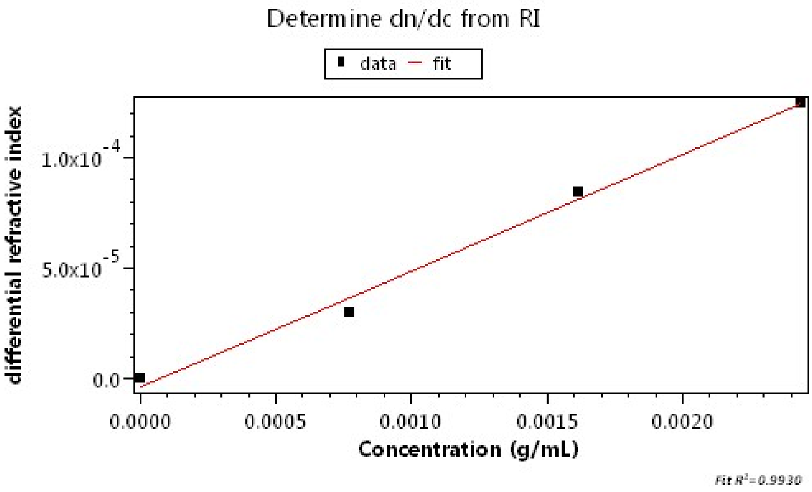

References

1. K. Nakano, K. Kobayashi and K. Nozaki, *J. Am. Chem. Soc.*, 2011, **133**, 10720-10723.
2. M. Mandal and D. Chakraborty, *J. Polym. Sci., Part A: Polym. Chem.*, 2015, **54**, 809-824.
3. C. C. Quadri and E. Le Roux, *Dalton Trans.*, 2014, **43**, 4242-4246.
4. J. Hessevik, R. Lalrempuia, H. Nsiri, K. W. Tornroos, V. R. Jensen and E. Le Roux, *Dalton Trans.*, 2016, **45**, 14734-14744.
5. C. Bakewell, G. Fateh-Iravani, D. W. Beh, D. Myers, S. Tabthong, P. Hormnirun, A. J. P. White, N. Long and C. K. Williams, *Dalton Trans.*, 2015, **44**, 12326-12337.
6. T. K. Saha, B. Rajashekhar and D. Chakraborty, *RSC Adv.*, 2012, **2**, 307-318.
7. J.-C. Buffet, A. N. Martin, M. Kol and J. Okuda, *Polym. Chem.*, 2011, **2**, 2378-2384.
8. H. C. Tseng, H. Y. Chen, Y. T. Huang, W. Y. Lu, Y. L. Chang, M. Y. Chiang, Y. C. Lai and H. Y. Chen, *Inorg. Chem.*, 2016, **55**, 1642-1650.
9. L. C. Liang, S. T. Lin and C. C. Chien, *Inorg. Chem.*, 2013, **52**, 1780-1786.
10. A. D. Schwarz, A. L. Thompson and P. Mountford, *Inorg. Chem.*, 2009, **48**, 10442-10454.
11. D. H. Wu, A. D. Chen and C. S. Johnson, *J. Magn. Reson. A*, 1995, **115**, 260-264.
12. SHELXTL, Bruker AXS, Madison, WI.
13. SHELX-2013 and G. M. Sheldrick, *Acta Cryst.*, 2015, **C71**, 3-8.